

DOI: 10.1002/cctc.201301009

# Key Mechanistic Insight into the Direct Gas-Phase Epoxidation of Propylene by the RuO<sub>2</sub>-CuO-NaCl/SiO<sub>2</sub> Catalyst

Anusorn Seubsai,<sup>\*,[a]</sup> Bahman Zohour,<sup>[b]</sup> Daniel Noon,<sup>[b]</sup> and Selim Senkan<sup>[b]</sup>

The discovery of the RuO<sub>2</sub>-CuO-NaCl/SiO<sub>2</sub> catalyst for the direct gas-phase epoxidation of propylene to propylene oxide created a potentially promising path towards developing a high-performing catalyst of substantial commercial value and opened a new challenge in catalysis research. In this work, studies following up this discovery are presented to reveal critical insight into the catalytic mechanism on the trimetallic catalyst. Small crystalline CuO particles, in close proximity of RuO<sub>2</sub>, were determined from temperature-programmed reduction and high-resolution transmission electron microscopy studies to be the site for propylene oxide synthesis. In addition, the presence of NaCl was confirmed to suppress the formation of CO<sub>2</sub>.

Propylene oxide (PO) is widely used in the preparation of various textiles and plastics<sup>[1]</sup> with over 8 million pounds of propylene-derived PO produced annually.<sup>[2]</sup> However, because some of the current production methods result in environmentally hazardous chlorinated byproducts that entail significant costs,<sup>[3]</sup> the search for an alternative method to achieve a high production rate of PO on an industrial scale has intensified. Although the direct gas-phase epoxidation of propylene to PO by molecular oxygen with the use of heterogeneous catalysts under atmospheric pressure is still, in theory, the most promising route, it has proven to be the most challenging production method thus far, as no breakthrough has yet been made.<sup>[3]</sup>

Several research groups have been exploring a number of alternatives, such as silver-based catalysts,<sup>[4]</sup> gold particles on titania with H<sub>2</sub> as a co-reactant,<sup>[5]</sup> titania-based catalysts,<sup>[6]</sup> molten salts of metal nitrates,<sup>[7]</sup> O<sub>3</sub> and nitrous oxide as reactants,<sup>[8]</sup> and copper-modified catalysts.<sup>[9,10]</sup> All of these methods suffer from low PO selectivities,<sup>[10–12]</sup> low propylene conversions,<sup>[5,10–14]</sup> short catalyst lifetimes,<sup>[6]</sup> high pressure requirements,<sup>[15]</sup> or costly co-reactants.<sup>[13,16]</sup> Consequently, no econom-

ically viable catalysts are currently available for the direct gas-phase epoxidation of propylene to PO by molecular oxygen.

Recently, we reported the discovery of RuO<sub>2</sub>-CuO<sub>x</sub>-NaCl/SiO<sub>2</sub> catalysts for the direct gas-phase epoxidation of propylene to PO that were prepared by the co-impregnation method.<sup>[17]</sup> It was shown that the catalyst system delivered a promising combination of PO selectivities (in the 40–50% range) and propylene conversions (10–20%) between 240 and 270 °C at atmospheric pressure. The best PO yield was obtained at a Ru/Cu/Na ratio of 4:2:1 at 12.5 wt% total metal loading on SiO<sub>2</sub>. Although the catalyst deactivated over time, as a result of the loss of chlorine content, we found that adding a small amount of a chlorocarbon (1–100 ppmv) such as chloroethane or 1,2-dichloroethane prevented deactivation by replenishing the chlorine content of the catalyst.<sup>[18]</sup> The chlorinated additives were found to play a critical role in maintaining high PO selectivities for at least 10 h under the conditions owing to geometric/ensemble and electronic effects, as well as gas-phase kinetic effects.

Herein, we report a critical key in understanding the mechanism of the epoxidation of propylene to PO facilitated by the SiO<sub>2</sub>-supported RuO<sub>2</sub>-CuO-NaCl catalyst by using oxygen as the only co-reactant. The desired propylene epoxidation reaction is shown in Equation (1).




However, the deep oxidation products CO<sub>2</sub> and H<sub>2</sub>O were also formed with the use of the title catalyst. Other detected trace byproducts included acetone (AT), acetaldehyde (AD), acrolein (AC), and propanal.

In earlier studies, the copper oxide phase was denoted as CuO<sub>x</sub>. However, recent XRD studies showed no evidence of Cu<sub>2</sub>O, which indicated the sole presence of CuO in the RuO<sub>2</sub>-CuO<sub>x</sub>-NaCl system. Given that the SiO<sub>2</sub>-supported RuO<sub>2</sub>-CuO-NaCl catalyst has multiple phases and contains more than one active metal, to understand the mechanism of propylene epoxidation to PO, the key active site for the formation of PO must first be identified. As reported earlier,<sup>[17]</sup> of the single catalyst systems (RuO<sub>2</sub>/SiO<sub>2</sub>, CuO/SiO<sub>2</sub>, and NaCl/SiO<sub>2</sub>), only CuO/SiO<sub>2</sub> produced detectable amounts of PO under the testing conditions, whereas the RuO<sub>2</sub>/SiO<sub>2</sub> catalyst led to complete combustion, and the NaCl/SiO<sub>2</sub> catalyst generally exhibited no activity. This implied that the CuO site may also be the key site for PO synthesis in our RuO<sub>2</sub>-CuO-NaCl system. To confirm this hypothesis, various catalytic materials were prepared and tested. The selectivity–conversion results of these catalysts are pre-

[a] Dr. A. Seubsai  
Department of Chemical Engineering, Faculty of Engineering  
Kasetsart University  
Ladyao, Jatujak, Bangkok, 10900 (Thailand)  
Fax: (+66) 02-561-4621  
E-mail: fengasn@ku.ac.th

[b] B. Zohour, D. Noon, Prof. Dr. S. Senkan  
Department of Chemical Engineering  
University of California  
Los Angeles, CA 90095 (USA)

 Supporting information for this article is available on the WWW under <http://dx.doi.org/10.1002/cctc.201301009>.

Catalyst #	Catalyst supported on SiO <sub>2</sub> <sup>[a]</sup>	Selectivity [%]					C <sub>3</sub> H <sub>6</sub> conversion [%]	PO yield [%]
		PO	AC	AT	AD	CO <sub>2</sub>		
ref.cat.	RuO <sub>2</sub> + CuO + NaCl	48	0	0	0	52	10.00	4.80
1	*RuO <sub>2</sub> + CuO + NaCl	40	0.5	0	0	60	6.25	2.48
2	*RuO <sub>2</sub> + CuO + Na <sub>2</sub> O	0	0	0	0	+ <sup>[b]</sup>	0.40	0
3	*RuO <sub>2</sub> + CuO	28	0.3	0	0	71.7	5.88	1.65
4	CuO + NaCl	0	0	0	0	+ <sup>[b]</sup>	0.05	0
5	CuO + Na <sub>2</sub> O	0	0	0	0	+ <sup>[b]</sup>	0.07	0
6	*RuO <sub>2</sub> + NaCl	1	0	0	0	99	5.39	0.04
7	*RuO <sub>2</sub> + Na <sub>2</sub> O	0	0	0	0	+ <sup>[b]</sup>	0.38	0
8	Na <sub>2</sub> O	0	0	0	0	+ <sup>[b]</sup>	0.08	0
9	NaCl	0	0	0	0	+ <sup>[b]</sup>	0.06	0

[a] Precursor: RuO<sub>2</sub> = (NH<sub>4</sub>)<sub>2</sub>RuCl<sub>6</sub>, \*RuO<sub>2</sub> = Ru(NO)(NO<sub>3</sub>)<sub>3</sub>, CuO = Cu(NO<sub>3</sub>)<sub>2</sub>·2.5H<sub>2</sub>O, NaCl = NaCl, Na<sub>2</sub>O = Na(NO<sub>3</sub>), weight ratio of Ru or \*Ru/Cu/Na/SiO<sub>2</sub> = 7.14:3.57:1.78:87.5. [b] In these very low C<sub>3</sub>H<sub>6</sub> conversion experiments, CO<sub>2</sub> was the only product observed. Measurements were taken with no chlorinated hydrocarbon co-feed after 2 h of startup if the catalyst performance remained in a pseudo-steady-state.

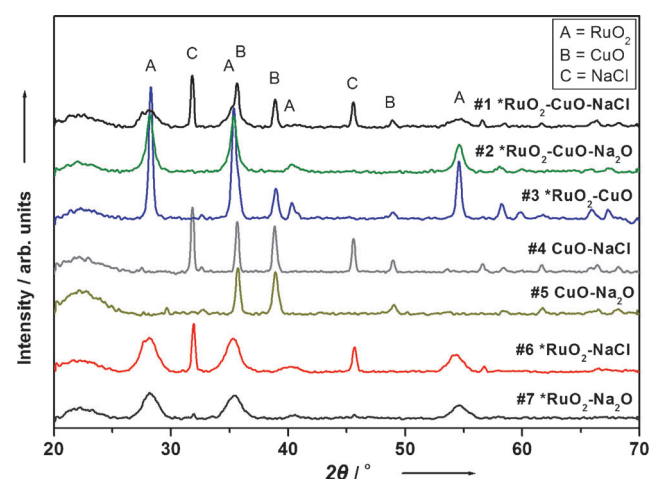


Figure 1. XRD spectra of the various catalysts investigated in this study.

sented in Table 1, and their XRD patterns are shown in Figure 1. The reference catalyst (ref.cat.) in Table 1 was prepared by using (NH<sub>4</sub>)<sub>2</sub>RuCl<sub>6</sub> as the RuO<sub>2</sub> precursor. To avoid residual chloride in the catalytic materials after calcination, Ru(NO)(NO<sub>3</sub>)<sub>3</sub> (denoted as \*RuO<sub>2</sub>, which has chemical activity similar to that of RuO<sub>2</sub>) was used as the source of Ru.

These results revealed several important aspects of this catalytic system, including the following:

- 1) Na<sub>2</sub>O (catalyst #8) and NaCl (catalyst #9) on SiO<sub>2</sub> were inactive for propylene reactions
- 2) The reference catalyst (ref.cat.) prepared from the (NH<sub>4</sub>)<sub>2</sub>RuCl<sub>6</sub> precursor provided a higher yield of PO than catalyst #1 prepared from the Ru(NO)(NO<sub>3</sub>)<sub>3</sub> precursor, because the excess amount of Cl (in the form of NaCl) promoted the formation of PO<sup>[18]</sup>
- 3) Importantly, Cl-free catalyst #2 exhibited very little reactivity with no PO formation. Comparison of the XRD spectra of catalysts #1 and #2 (Figure 1) also showed that the crystalline CuO phase (indicated by B) in catalyst #1 was absent in

catalyst #2, which was Cl free. This is important evidence that suggests that CuO crystals are the key catalytic sites for the synthesis of PO in this system

- 4) Comparison of the XRD spectra of catalysts #1, #2, #4, and #5 revealed that only catalyst #2 did not show the crystalline CuO phase peak at 2θ = 39°. This suggests that in the absence of Cl ions but in the presence of Ru, Cu, and Na ions, the Na ions block the formation of CuO crystals
- 5) Comparison of the reactivity results in Table 1 for catalysts #2, #5, and #7 revealed that Na<sub>2</sub>O strongly inhibited the reaction. Na ions also appear to have reduced the particle size of RuO<sub>2</sub>, as seen by comparing the XRD spectrum of catalyst #3 to the spectra of #1, #2, #6, and #7 at approximately 26–28°. However, because the \*RuO<sub>2</sub> peaks become broader, especially for catalyst #1, this appears also to improve the PO selectivity
- 6) Comparison of catalysts #6 and #7 in Table 1 revealed that NaCl is important not only to suppress the formation of CO<sub>2</sub><sup>[18]</sup> but also to initiate the reaction. Catalyst #6 gave higher conversions of propylene than catalyst #7, but the product was primarily CO<sub>2</sub>
- 7) Comparison of catalysts #4 and #6 revealed that NaCl plays a critical role only in the presence of both \*RuO<sub>2</sub> and CuO. This indicates that \*RuO<sub>2</sub> is also an active catalytic site but for the complete combustion
- 8) Comparison of catalysts #1 and #6 revealed that these two samples exhibited similar conversions of propylene but visibly different PO selectivities, which clearly points to CuO as an important site for the transformation of propylene into PO after initial activation over \*RuO<sub>2</sub> crystals. This indicates a cooperative effect between \*RuO<sub>2</sub> and the CuO crystals. In contrast, catalyst #3 indicates that even in the absence of the Cl source, CuO and RuO<sub>2</sub> may cooperate and convert propylene into PO, but with lower PO selectivity.

In summary, for the SiO<sub>2</sub>-supported RuO<sub>2</sub>-CuO-NaCl catalysts, crystalline CuO is implicated as the main catalytic site for the formation of PO with promotion by crystalline RuO<sub>2</sub> and CO<sub>2</sub> suppression by NaCl. To test this hypothesis, a series of experiments were performed to study the effects of the NaCl loading on the RuO<sub>2</sub>-CuO/SiO<sub>2</sub> catalysts. The catalysts were prepared by using (NH<sub>4</sub>)<sub>2</sub>RuCl<sub>6</sub>, Cu(NO<sub>3</sub>)<sub>2</sub>·2.5H<sub>2</sub>O, and Na(NO<sub>3</sub>) as precursors, followed by impregnation on SiO<sub>2</sub>, drying, and calcination as described earlier. It was also assumed, for calculation purposes, that all Na atoms would form crystalline NaCl in the final materials as a result of the excess amount of the Cl source. The performance test results of this series of catalysts are shown in Figure 2.

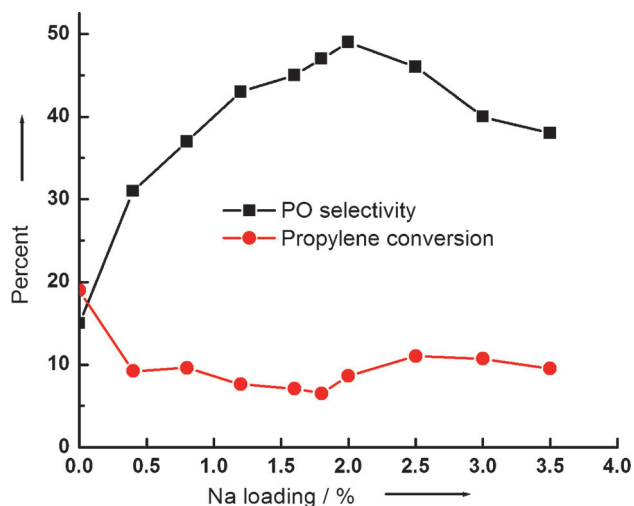


**Figure 2.** Results of the  $\text{RuO}_2\text{-CuO/SiO}_2$  catalysts at different Na loadings. Precursor:  $\text{RuO}_2 = (\text{NH}_4)_2\text{RuCl}_6$ ,  $\text{CuO} = \text{Cu}(\text{NO}_3)_2 \cdot 2.5\text{H}_2\text{O}$ ,  $\text{Na}_2\text{O} = \text{Na}(\text{NO}_3)$ , weight ratio  $\text{Ru/Cu} = 7.14:3.57$ ,  $\text{SiO}_2$  and Na were varied. Measurements were taken with no chlorinated hydrocarbon co-feed after 2 h of startup if the catalyst performance remained in a pseudo-steady-state.

As seen in Figure 2, in the absence of Na loading, propylene conversion was approximately 19% with a PO selectivity of 15%. Increasing the Na loading to 2% increased the PO selectivity to a maximum of approximately 49%, whereas the conversion of propylene decreased to approximately 9%. At higher Na loadings, the PO selectivity started to decrease, whereas the conversion of propylene remained relatively constant at approximately 10%.

At low Na loadings, the NaCl crystals are expected to be well dispersed and small, and they could even be incorporated into the solid structure. They also primarily occupy highly acidic sites on the catalysts, which causes  $\text{CO}_2$  suppression. This initially results in lower conversions of propylene, but increased PO selectivity owing to electronic effects.<sup>[18]</sup> After all of the highly acidic sites are capped, however, the remaining Na (as NaCl) forms larger NaCl crystals and/or aggregates. After a certain point ( $\approx 2\%$  Na loading in our experiments, Figure 2), the excess amount of NaCl leads to the formation of larger crystals, which then separate from the  $\text{RuO}_2\text{-CuO}$  clusters; this lowers the PO selectivity, whereas the conversion of propylene remains approximately the same. The XRD spectra of this group of catalysts confirmed this explanation (see the Supporting Information).

A temperature-programmed reduction (TPR) experiment was also performed to gain insight into the nature and interaction of the surface sites, especially for  $\text{RuO}_2$  and CuO (see Figure 3). The TPR profile of  $\text{CuO/SiO}_2$  shows a single broad peak at  $423^\circ\text{C}$ , whereas that for catalyst #4 shows two peaks: a main peak at  $423^\circ\text{C}$  and a shoulder at approximately  $330^\circ\text{C}$ . The peak at  $423^\circ\text{C}$  is due to the reduction of bulk CuO, and the lower-temperature peak corresponds to the reduction of the highly dispersed copper species (e.g., small 2D or 3D clusters), including isolated  $\text{Cu}^{2+}$  ions that interact with the  $\text{SiO}_2$  support.<sup>[19]</sup> As seen in Figure 3, all  $\text{RuO}_2$ -containing catalysts exhibit two TPR peaks. The peak at the lower temperature (be-

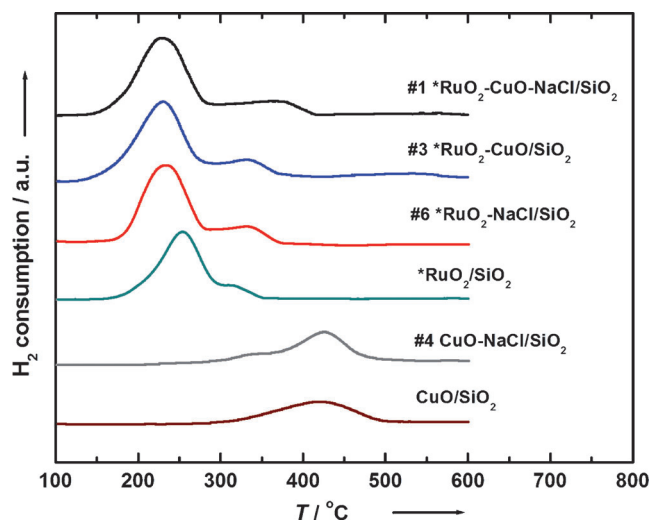


**Figure 3.** TPR profiles of all combinations of  $\text{RuO}_2$ , CuO, and NaCl on  $\text{SiO}_2$ . Each catalyst had a weight percent of Ru, Cu, and Na on  $\text{SiO}_2$  of 7.19, 3.57, and 1.79%, respectively.

tween  $230$  and  $250^\circ\text{C}$ ) corresponds to the complete reduction of  $\text{Ru}^{4+}$  to  $\text{Ru}^0$ , and the shoulder ( $\approx 320^\circ\text{C}$ ) corresponds to the ruthenium species interacting with the support.<sup>[20]</sup> Mass spectrometric monitoring of the effluent gases during the TPR experiments revealed no  $\text{CO}_x$  or  $\text{CH}_4$ .<sup>[21]</sup> This suggests that the above explanations for the observed TPR shoulders are likely correct.

A close inspection of the TPR profiles in Figure 3 revealed that the maximum peak for catalysts #1 and #6 was shifted towards lower temperatures relative to that of  $\text{RuO}_2/\text{SiO}_2$ , that is, from  $253$  to  $230^\circ\text{C}$ . In contrast, the shoulder was shifted towards higher temperatures, that is, from  $310^\circ\text{C}$  for the  $\text{RuO}_2/\text{SiO}_2$  catalyst to  $370$  and  $350^\circ\text{C}$  for catalyst #1 and #6, respectively. These shifts may be due to a decrease in the size of the  $\text{RuO}_2$  particle in the presence of Na. A similar trend was also observed for the TPR profile of catalyst #3 relative to that of  $\text{RuO}_2/\text{SiO}_2$ . In this case, a combination of effects may be responsible for the observed TPR shifts. First, the particle size of  $\text{RuO}_2$  in catalyst #3 is smaller than that in  $\text{RuO}_2/\text{SiO}_2$  as a consequence of the presence of CuO.<sup>[17]</sup> Second, the observed shifts can be due to the presence of strong interactions between  $\text{RuO}_2$  and the CuO crystals.

As mentioned above, the main TPR peaks were at  $423^\circ\text{C}$  for CuO in catalyst #4 and  $\text{CuO/SiO}_2$ . However, such peaks were absent in other CuO-containing catalysts such as catalysts #1 and #3. This is because both  $\text{RuO}_2$  and CuO were reduced simultaneously in catalysts #1 and #3 owing to a spillover effect induced by the rapid reduction of  $\text{RuO}_2$ . That is, at lower temperatures the  $\text{RuO}_2$  TPR peak becomes larger, which is caused by a larger consumption of  $\text{H}_2$ <sup>[22]</sup> by the combined reduction of  $\text{RuO}_2$  and CuO, concomitant with the loss of the individual CuO peak at higher temperatures. This phenomena was also observed in the study of the Ru-Cu system for butane hydrogenolysis.<sup>[20]</sup> That study concluded that CuO was well spread on the surface of  $\text{RuO}_2$  and that  $\text{RuO}_2$  and CuO were in very close proximity. Our TPR results presented in Figure 3 are in

harmony with this picture. A close inspection of the TPR profile for catalyst #3 revealed the presence of a very small and broad peak at approximately 500 °C. This could be due to some isolated CuO clusters that remained on the SiO<sub>2</sub> surface that were distant from the RuO<sub>2</sub> crystals in the absence of Na.

Shown in Figure 4 is a high-resolution transmission electron microscopy (HR-TEM) image in support of the TPR experiments. Although it is difficult to identify the small CuO crystals (3–5 nm) on the surface of the RuO<sub>2</sub> crystals ( $\approx 10 \times 30$  nm), the use of a crystal plane unique (fast Fourier transform) to RuO<sub>2</sub> and CuO can identify these components. The TEM images also

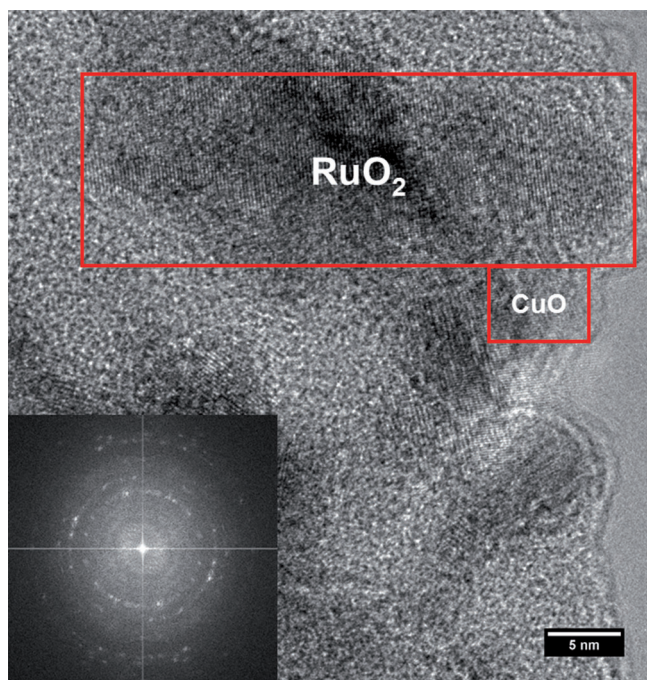


**Figure 4.** HR-TEM image of the SiO<sub>2</sub>-supported RuO<sub>2</sub>-CuO-NaCl catalyst. The RuO<sub>2</sub>+CuO clusters are in close proximity. Fast Fourier transform of the HR-TEM image was used to identify crystal planes unique to RuO<sub>2</sub>, CuO, and NaCl.

confirmed that CuO and RuO<sub>2</sub> were distinct crystal structures that were in close proximity. Notably, NaCl crystals were also present as cubic structures ( $\approx 30$  nm) but are not shown in this particular TEM image.

By taking into account all of the aforementioned findings, a model for the RuO<sub>2</sub>-CuO-NaCl/SiO<sub>2</sub> catalyst and a plausible mechanism for the epoxidation of propylene over this catalyst system may be formulated. The proposed model and mechanism are shown in Figure 5a,b. According to this mechanism, an O<sub>2</sub> molecule first adsorbs (chemisorption) onto an active center on the RuO<sub>2</sub> surface and dissociates into two surface O atoms (O<sub>s</sub>). The O<sub>s</sub> migrates across the surface to a neighboring CuO site, which is in close proximity, to form CuO–O. Gas-phase propylene then interacts with CuO–O ultimately to form PO through the formation of relevant intermediates such as an oxametallocycle and other species.<sup>[23]</sup>

In conclusion, a mechanism for the direct epoxidation of propylene by O<sub>2</sub> over a SiO<sub>2</sub>-supported RuO<sub>2</sub>-CuO-NaCl cata-

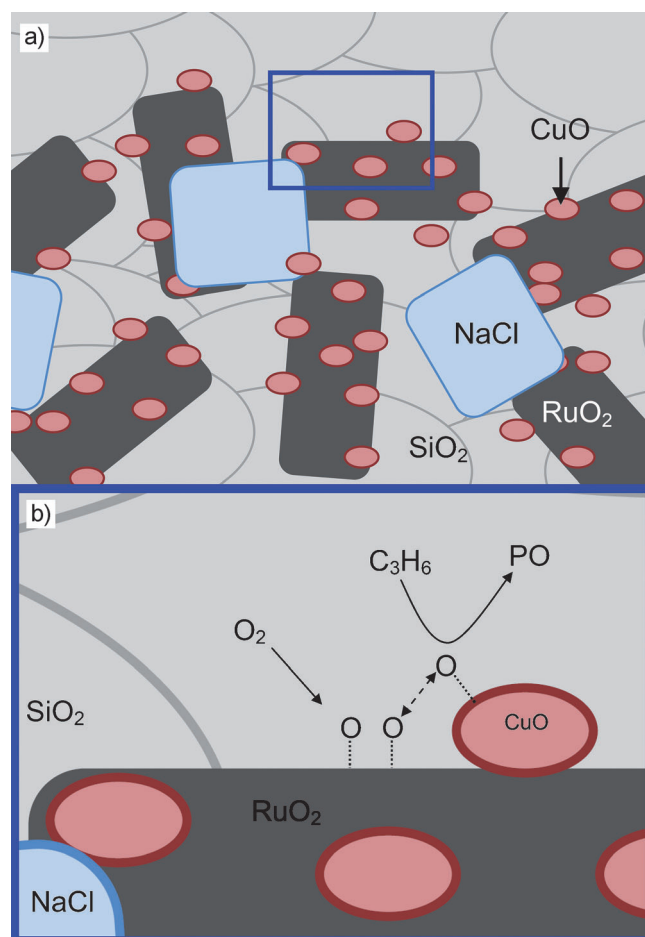


**Figure 5.** a) Schematic structure of the RuO<sub>2</sub>-CuO-NaCl/SiO<sub>2</sub> catalyst. b) Proposed mechanism for the epoxidation of propylene, showing the dissociative adsorption of O<sub>2</sub> onto the RuO<sub>2</sub> surface, surface migration of adsorbed oxygen to CuO surface, and the formation of PO.

lyst, previously discovered in our laboratories, was developed. The trimetallic catalyst at 12.5 wt% total metal loading was characterized by using powder XRD, HR-TEM, and TPR techniques. These studies confirmed that this catalyst system consists of distinct nanocrystals of RuO<sub>2</sub>, CuO, and NaCl. Furthermore, the crystalline RuO<sub>2</sub> and CuO particles are in close proximity, and the CuO particles are generally smaller than the RuO<sub>2</sub> particles with the result that the CuO particles are likely to be positioned on the surface of the RuO<sub>2</sub> structures. In investigations of the effects of Na and Cl, Na<sub>2</sub>O showed itself to be a strong inhibitor of PO synthesis, whereas NaCl played two important roles: it reduced the RuO<sub>2</sub> crystal size, which favored PO activity,<sup>[17]</sup> and suppressed CO<sub>2</sub> combustion, which led to higher PO selectivity. A critical finding ascertained from comparing the XRD patterns and the performance test results of single and bimetallic subsets of the RuO<sub>2</sub>-CuO-NaCl/SiO<sub>2</sub> catalyst, along with chlorinated and unchlorinated variants, indicated that the active site of the catalyst is likely the CuO crystal. A mechanism was therefore proposed in which RuO<sub>2</sub> adsorbs diatomic oxygen from the gas phase; then, the adsorbed oxygen undergoes surface migration onto CuO, from which it is transferred to propylene to form PO. Further improvements of this

catalyst thus could be made by precise arrangement of the crystalline RuO<sub>2</sub>, CuO, and NaCl phases on the SiO<sub>2</sub> support.

## Experimental Section

SiO<sub>2</sub>-supported mono-, bi-, and trimetallic heterogeneous catalysts were prepared by co-impregnation. For the monometallic catalysts, the metal salt aqueous solutions with aqueous solution mixtures of Ru [(NH<sub>4</sub>)<sub>2</sub>RuCl<sub>6</sub>, Aldrich or Ru(NO)(NO<sub>3</sub>)<sub>3</sub>, Alfa Aesar, Ru 31.3% min], Cu [Cu(NO<sub>3</sub>)<sub>2</sub>·2.5H<sub>2</sub>O, Alfa Aesar, ACS, 98.0–102.0%], and Na (NaNO<sub>3</sub>, Alfa Aesar, ACS, 99.0% or NaCl, Alfa Aesar ACS, 99%)<sup>[24]</sup> were prepared to achieve a predetermined weight percent (by metal atomic weight) loading on the SiO<sub>2</sub> support powder (SiO<sub>2</sub>, Alfa Aesar, surface area 145 m<sup>2</sup>g<sup>-1</sup>). Each metal salt solution was introduced to SiO<sub>2</sub> and left to penetrate the support for 24 h in air. The resulting materials were dried (120 °C, until dry) and calcined (500 °C, 12 h) in air.

These materials (≈5.0 mg.) were investigated for their catalytic performance by using previously developed high-throughput heterogeneous catalysis screening tools.<sup>[25]</sup> The array channel reactor was used to test 80 different catalysts in a single experiment by using a computer-controlled system. All experiments were performed under atmospheric pressure at a gas hourly space velocity of 20 000 h<sup>-1</sup> controlled by using mass flow controllers (MKS, Andover, MA). The feed gas consisted of 1 vol% propylene (C<sub>3</sub>H<sub>6</sub>), 4 vol% O<sub>2</sub>, and balance He at a reactor temperature of 250 °C. Data analysis was conducted by an online Micro-Gas Chromatograph (Varian, CP-4900) equipped with a thermal conductivity detector (TCD), Porapak U (10 m), and 5 Å molecular sieves (10 m). The detected products were propylene oxide, acetone, acetaldehyde, CO<sub>2</sub>, and acrolein. The propylene conversion, product selectivity, and yield (calculated as selectivity of a product × propylene conversion) of the products were determined on the basis of carbon balance. The reproducibility of the experiments was within ±10%.

Powder XRD patterns were obtained with an X-ray powder diffractometer (Panalytical X'Pert Pro) by using CuK<sub>α</sub> radiation, 45 kV, and 40 mA to identify different phases. TEM studies were performed by using a FEI Titan 80-300 TEM. For high-resolution TEM imaging a field emission gun operating at 300 kV was used.

TPR measurements were made by using an apparatus developed in the laboratory.<sup>[26]</sup> Each TPR run was performed by passing a H<sub>2</sub>-He mixture (5% H<sub>2</sub>) over the catalyst (160 mg) placed in a quartz reaction tube (0.8 cm in diameter and 45 cm long) positioned in a furnace (Vulcan 3-550) at a total gas flow rate of 20 mLmin<sup>-1</sup>. A heating rate of 10 °Cmin<sup>-1</sup> was set by using the furnace's programmable temperature controller (PID). Hydrogen consumption was monitored online by a quadruple mass spectrometer (QMS, RGA 200, Stanford Research System, Santa Clara, CA) from 100 to 600 °C. Prior to the TPR measurements, the catalysts were treated in situ by flowing He at 20 mLmin<sup>-1</sup> from RT to 200 °C at a heating rate of 10 °Cmin<sup>-1</sup> and maintaining these conditions for an additional 1 h, after which it was cooled down to 100 °C.

## Acknowledgements

We thank the Laboratory Catalyst Systems, LLC, for providing access to their facilities, for the use of their catalytic materials discovery library, and for financial support. A.S. acknowledges the Faculty of Engineering, Kasetsart University for financial support.

B.Z. acknowledges the University of California, Los Angeles (UCLA) Graduate Division Fellowship. D.N. acknowledges the National Science Foundation MCTP-DGE-0654431.

**Keywords:** copper oxide · epoxidation · propylene oxide · ruthenium oxide · supported catalysts

- [1] D. Kahlich, U. Wiechern, J. Lindner, *Propylene Oxide*. In *Ullmann's Encyclopedia of Industrial Chemistry*, Wiley, 2000, pp. 1–25.
- [2] F. Cavani, J. H. Teles, *ChemSusChem* 2009, 2, 508–534.
- [3] T. A. Nijhuis, M. Makkee, J. A. Moulijn, B. M. Weckhuysen, *Ind. Eng. Chem. Res.* 2006, 45, 3447–3459.
- [4] R. A. Vansanten, C. P. M. Degroot, *J. Catal.* 1986, 98, 530–539.
- [5] T. Hayashi, K. Tanaka, M. Haruta, *J. Catal.* 1998, 178, 566–575.
- [6] K. Murata, Y. Kiyozumi, *Chem. Commun.* 2001, 1356–1357.
- [7] T. A. Nijhuis, S. Musch, M. Makkee, J. A. Moulijn, *Appl. Catal. A* 2000, 196, 217–224.
- [8] a) S. Yang, W. Zhu, Q. Zhang, Y. Wang, *J. Catal.* 2008, 254, 251–262; b) X. X. Wang, Q. H. Zhang, S. F. Yang, Y. Wang, *J. Phys. Chem. B* 2005, 109, 23500–23508.
- [9] a) W. M. Zhu, Q. H. Zhang, Y. Wang, *J. Phys. Chem. C* 2008, 112, 7731–7734; b) H. Chu, L. Yang, Q. H. Zhang, Y. Wang, *J. Catal.* 2006, 241, 225–228; c) Y. Wang, H. Chu, W. Zhu, Q. Zhang, *Catal. Today* 2008, 131, 496–504.
- [10] O. P. H. Vaughan, G. Kyriakou, N. Macleod, M. Tikhov, R. M. Lambert, *J. Catal.* 2005, 236, 401–404.
- [11] Z. Song, N. Mimura, J. J. Bravo-Surez, T. Akita, S. Tsubota, S. T. Oyama, *Appl. Catal. A* 2007, 316, 142–151.
- [12] J. H. Huang, T. Akita, J. Faye, T. Fujitani, T. Takei, M. Haruta, *Angew. Chem. Int. Ed.* 2009, 48, 7862–7866; *Angew. Chem.* 2009, 121, 8002–8006.
- [13] T. Hayashi, L. B. Han, S. Tsubota, M. Haruta, *Ind. Eng. Chem. Res.* 1995, 34, 2298–2304.
- [14] a) B. S. Uphade, M. Okumura, S. Tsubota, M. Haruta, *Appl. Catal. A* 2000, 190, 43–50; b) A. K. Sinha, S. Seelan, S. Tsubota, M. Haruta, *Angew. Chem. Int. Ed.* 2004, 43, 1546–1548; *Angew. Chem.* 2004, 116, 1572–1574.
- [15] H. Orzesek, R. P. Schulz, U. Dingerdissen, W. F. Maier, *Chem. Eng. Technol.* 1999, 22, 691–700.
- [16] M. Daté, Y. Ichihashi, T. Yamashita, A. Chiorino, F. Boccuzzi, M. Haruta, *Catal. Today* 2002, 72, 89–94.
- [17] A. Seubsai, M. Kahn, S. Senkan, *ChemCatChem* 2011, 3, 174–179.
- [18] A. Seubsai, S. Senkan, *ChemCatChem* 2011, 3, 1751–1754.
- [19] Z. L. Wang, Q. S. Liu, J. F. Yu, T. H. Wu, G. J. Wang, *Appl. Catal. A* 2003, 239, 87–94.
- [20] S. Galvagno, C. Crisafulli, R. Maggiore, G. R. Tauszik, A. Giannetto, *J. Therm. Anal.* 1985, 30, 611–618.
- [21] D. E. Damiani, E. D. P. Millan, A. J. Rouco, *J. Catal.* 1986, 101, 162–168.
- [22] M. G. Musolino, C. V. Caia, C. Busacca, F. Mauriello, R. Pietropaolo, *Appl. Catal. A* 2009, 357, 106–113.
- [23] a) L. J. Broadbelt, R. Q. Snurr, *Appl. Catal. A* 2000, 200, 23–46; b) D. Torres, N. Lopez, F. Illas, R. M. Lambert, *Angew. Chem. Int. Ed.* 2007, 46, 2055–2058; *Angew. Chem.* 2007, 119, 2101–2104.
- [24] A. C. Kizilkaya, S. Senkan, I. Onal, *J. Mol. Catal. A* 2010, 330, 107–111.
- [25] a) S. Duan, S. Senkan, *Ind. Eng. Chem. Res.* 2005, 44, 6381–6386; b) S. M. Senkan, S. Ozturk, *Angew. Chem. Int. Ed.* 1999, 38, 791–795; *Angew. Chem.* 1999, 111, 867–871; c) S. Senkan, K. Krantz, S. Ozturk, V. Zengin, I. Onal, *Angew. Chem. Int. Ed.* 1999, 38, 2794–2799; *Angew. Chem.* 1999, 111, 2965–2971; d) S. Senkan, M. Kahn, S. Duan, A. Ly, C. Leidhom, *Catal. Today* 2006, 117, 291–296; e) S. Senkan, *Angew. Chem. Int. Ed.* 2001, 40, 312–329; *Angew. Chem.* 2001, 113, 322–341.
- [26] A. Miller, B. Zohour, A. Seubsai, D. Noon, S. Senkan, *Ind. Eng. Chem. Res.* 2013, 52, 9551–9555.

Received: November 28, 2013

Revised: January 20, 2014

Published online on April 1, 2014